Low-cost Li$_2$S-based cathode for lithium sulfur battery

Hamid Mollania, Majid Oloomi-Buygi*

Ferdowsi University of Mashhad, Department of Electrical Engineering, Mashhad, Iran.

*Corresponding author email: m.oloomi@um.ac.ir

ABSTRACT

Low-cost lithium-sulfur batteries (LSBs) with high specific energy density have drawn the attention of the industrial community as lithium-ion batteries get closer to their theoretical limits. However, their commercialization is constrained by the use of lithium metal anodes and the shuttle effect of lithium polysulfides (LiPSs) in redox processes. Ketjenblack (KB) was used in this research work to embed cobalt nanoparticles with a diameter smaller than 40 nm in order to create a suitable and affordable cathode host. Incorporating Co nanoparticles with KB that has a porous structure and great electrical conductivity allows the host to confine LiPSs chemically and physically, which is beneficial for lowering the shuttle effect and lengthening the lifespan of LSBs. Additionally, by using the lithiated form of sulfur (Li$_2$S) rather than sulfur as the cathode material, the lithium source was moved from the anode to the cathode, reducing the safety concerns related to Li metal anodes and enabling the use of non-metallic anode materials like silicon and tin in LSBs. Li$_2$S-Co@KB cathode has an initial discharge capacity of 850.3 $\mathrm{mAhg_{Li2S}}^{-1}$. The cell has shown strong cycling stability at a 0.5 C current rate for over 300 cycles, with low capacity fading of 0.19% per cycle, as well as exceptional C-rate performances up to 5 C.

Keywords: *Lithium–sulfur battery, lithium sulfide, polysulfides, low-cost, sulfur cathode.*

1. Introduction

Renewable energies such as wind and solar are inherently intermittent, efficient dispatching of these energy sources requires attention to eco-friendly storage devices. Among the energy storage devices, Lithium-ion batteries (LIBs) bring practical solutions to the significant challenges of integrating intermittent energy sources into a smart renewable-based grid and electric vehicles. LIBs have approached their theoretical limit that cannot satisfy the increasing demand for high energy density storage devices [1,2].

Over the past ten years, interest in lithium-sulfur batteries as high-energy-density electrochemical energy storage devices has increased significantly. Sulfur, has a high theoretical specific capacity density (1675 mAh g^{-1}), and low environmental impact [3,4]. In addition to their potential advantages, LSBs also have several key challenges that prevent them from practical applications. Low electrical and ionic conductivity of sulfur, poor redox kinetics, and shuttle effect resulted from soluble long-chain polysulfides (LiPSs) (Li$_2$S$_x$, $4 \leq x \leq 8$) decrease the battery power density and life span [5,6]. Besides that, utilizing metallic lithium as anode prevents LSBs from being commercialized. Using lithium sulfide (Li$_2$S) as an alternative to sulfur with a high specific capacity of 1166 mAh g^{-1} and a melting

point of 938 °C, can solve the safety concerns related to metallic Li anodes. Besides the benefits, even with Li_2S cathodes, the LSBs still have some drawbacks, such as low electrical and ionic conductivity of Li_2S, and the LiPSs shuttle effect [7,8]. Furthermore, commercial Li_2S has low ionic conductivity, and activating Li_2S causes a high potential barrier (around 1 V) in the initial charge process of Li_2S [9]. Therefore, to solve the issues and maximize the utilization of Li_2S during cycling, in addition to reducing the size of the Li_2S particle, the Li_2S host requires a proper design to increase electronic and ionic conductivities and mitigate the impacts of soluble polysulfides [10]. Carbon-based matrices can physically block LiPSs while also greatly increasing the cathode composite's electrical conductivity and provides a conductive framework that facilitates the movement of electrons throughout the material; however, because of their non-polar surface, their interactions with LiPSs are poor, which causes a continuous loss of active material throughout the cycling [11]. Several carbonaceous materials such as carbon nanofibers [12], carbon nanotubes [13], and mesoporous carbon [14] have been reported to enclose the Li_2S nanoparticles. Coating the carbon-based substrates with catalyst like Co could trap LiPSs by the abundant chemisorption sites that can improve the characteristic of carbon structures in absorbing polysulfides and create additional conductive pathways within the composite [15,16]. Covering Ketjenblack (KB), hollow ball type of carbon-based substrate, with high specific surface area and hollow morphology by cobalt nanoparticles in addition to increase the conductivity of the host, can also solve the aggregation problem of cobalt nanoparticles.

Herein, by using a facile method, the Co nanoparticles are decorated on the KB. The Co@KB composite was then covered by Li_2S nanoparticles with a simple infiltration and evaporation approach. As-synthesized Co@KB and Li_2S-Co@KB composites were characterized with different techniques. The LiPS adsorption ability of the Co@KB host was evaluated. Furthermore, the cycle stability and rate capability of the Li_2S-Co@KB cathode were investigated by assembling half cells.

2. Materials and methods
2.1. Synthesis of Co@KB and Li_2S-Co@KB composites
To synthesize Co@KB, typically we used 1.3 g of KB and 1.3 g of Cobalt (II) nitrate dispersed in deionized water and after stirring for 12 hours, the mixture was transferred inside the fume hood to dry under the medium vacuum level for a night. Afterward, the powder was carbonized under 800 °C for 5 h under an Ar atmosphere to convert to the Co@KB composite. To synthesize the Li_2S-Co@KB a solution of commercial Li_2S and absolute ethanol (0.5 M), infiltered to the 73 mg of Co@KB composite and under 100 °C using an oil bath the solvent evaporated, and the final composite after drying during the night was used as the active cathode material. The Li_2S content in Li_2S-Co@KB was around 61 wt.%.

2.2. Characterization
XRD measurements were carried out on a Bruker AXS diffractometer with Cu-Kα radiation (λ = 1.5406 Å) from 20 to 80° operating at 40 kV. The morphology of samples was examined by the Scanning Electron Microscope (SEM) coupled with INCA instruments Energy Dispersive X-ray spectrometer (EDX). N_2 adsorption-desorption isotherms on a TriStar II 3020 Micromeritics surface area analyzer were used to determine the samples' specific surface area.

2.3. Electrochemical measurements
For testing the cathode material, we used Li metal as a counter electrode, and the mixture of Li_2S-Co@KB/conductive carbon/PVDF (8/1/1) was fabricated as the cathode. Also, a Celgard 2500 membrane was used as the separator, which was soaked in 1.0 M LiTFSI, 1,2-dimethoxy ethane (DME), 1,3-dioxolane (DOL) (v/v = 1/1), and 0.1 M $LiNO_3$ as an electrolyte. All the cell assembly was done inside the glove box. The cells were cycled at a voltage window of 1.7–3.6 V for the first cycle and 1.7–2.8 V for the other cycles on a Neware battery tester.

3. Results
As shown in Fig. 1, the Li_2S-Co@KB composite was synthesized by introducing the fine Li_2S nanoparticles to the Co@KB host by a simple liquid infiltration-evaporation approach, following the initial dispersion of Co nanoparticles into the Ketjenblack (KB).

Fig. 2a shows the powder X-ray diffraction (XRD) patterns of Co@KB; the first two main diffraction peaks are belonged to the KB, and the next three peaks are related to the crystalline planes of Co nanoparticles. Based on N_2 adsorption-desorp-

tion isotherms, the specific surface area (SSA) of the Co@KB sample has been established (Fig. 2b). The Co@KB sample displays an apparent capillary condensation phenomenon along with a classic type IV adsorption-desorption curve. A type H3 hysteresis loop is visible in the adsorption-desorption isotherms between 0.42 and 1 relative pressure [9,13]. Co@KB has a Brunauer–Emmett–Teller (BET) SSA of 970.5 m^2g^{-1} and a Barret-Joyner-Halenda (BJH) pore volume of 2.1 cm^3g^{-1}. This high SSA and pore space are advantageous for the nucleation of Li_2S particles.

Scanning electron microscopy (SEM) images of the Co@KB composite with different magnifications is shown in Fig. 3a. The metallic Co nanoparticles can be clearly seen as brighter points in the SEM image. The average diameter of Co nanoparticles is below 40 nm. As the KB soaked well with Co precursor and dried slowly before carbonization, it can be seen that the Co nanoparticles were distributed and embedded well in the porous structure of the KB substrate. Furthermore, to confirm the existence of Co nanoparticles, the SEM-energy dis-

persive X-ray spectroscopy (EDX) analysis was also investigated.

To be able to get clear results for SEM analysis, first, the Co@KB composite was dispersed well in hexane solvent, and the mixture was drop-cast on the single silicon wafer substrate before analysis. Fig. 3b shows the SEM image and corresponding EDX spectrum of the Co@KB composite. EDX results show the presence of carbon and cobalt in the structure. In LSBs, the high surface area of the active material of the electrodes can increase their contact with the electrolyte. Introducing the Co nanoparticles to the substrate can decrease the surface area, but by using substrates like KB that normally have high surface areas, even after decorating with Co nanoparticles, the surface area is still high, which is good for uniform distribution of Li_2S into the host. Fig. 3c demonstrates Li_2S-Co@KB after introducing it into the host material. The EDX result also confirms the presence of S, C, and Co in the structure. The conductivity of Co is higher than KB, so introducing Co nanoparticles can enhance the total electrochemical performance of
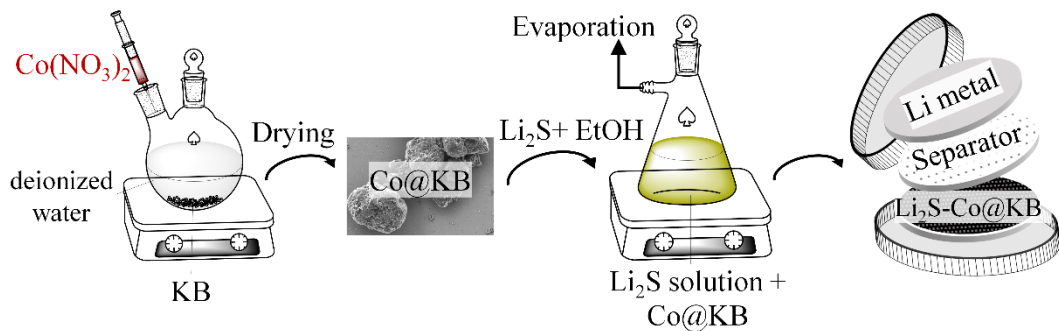
Fig. 1- Schematic of the Li_2S-Co@KB preparation method and configuration of cell components in the assembled coin-type cells.
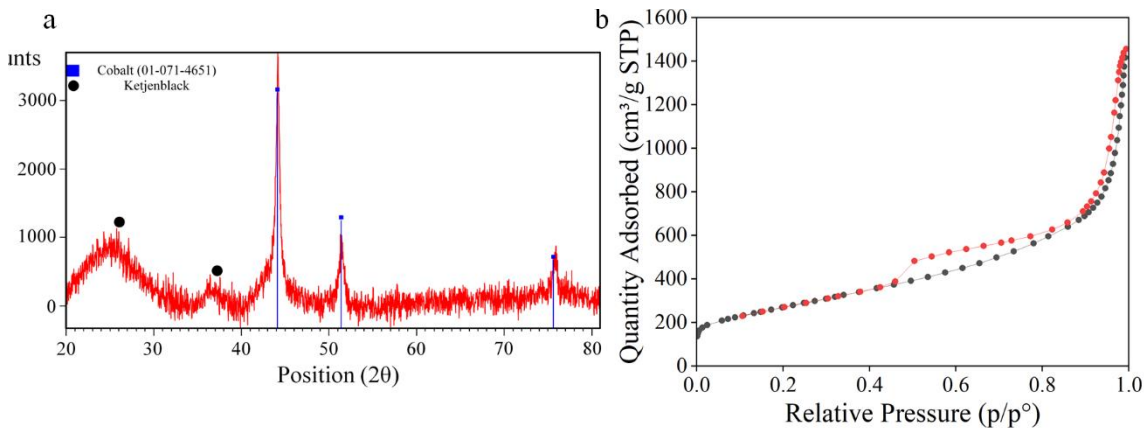
Fig. 2- (a) XRD patterns of Co@KB composite (b) N_2 adsorption.

the cathode.

During the discharge, lithium metal is oxidized, and lithium ions move to the cathode through the electrolyte and form Li–S compounds. On the cathode side, firstly, the S_8 is reduced to Li_2S_4, and secondly, Li_2S_4 will be further reduced to Li_2S to complete the discharge process. The discharge reaction equations are mentioned as follows [17]:

Anode: $16Li \rightarrow 16Li^+ + 16e^-$ (1)

Cathode (Short-chain LiPS): $S_8 + 4Li^+ + 4e^- \rightarrow 2Li_2S_4$ (2)

(Long-chain LiPS): $2Li_2S_4 + 12Li^+ + 12e^- \rightarrow 8Li_2S$
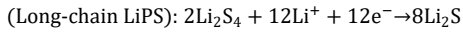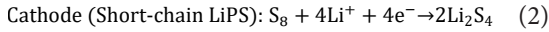
As described above, the discharge process of LSB in an ether-based electrolyte is a successive process, and during the transformation of S to Li_2S, some intermediate, called polysulfides (Li_2S_x), will be produced. If the host is not able to trap the polysulfide, this unwanted intermediate will move to the anode and will react with the metallic anode, causing some safety concerns. In the Co@KB composite, the porous and hollow structure of KB can make the movement of lithium ions easier and also physically trap the polysulfides. The Co nanoparticles, which can chemically trap the polysulfides, improve the trapping of polysulfides in the cathode structure. Aside from the catalytic impact, Co nanoparticles improve the host's electrical conductivity and can significantly reduce the overpotential barrier of Li_2S activation in the first charge cycle, resulting in lower capacity fading and a longer cycle life. The LiPS adsorption capability of Co@KB was optically shown in Fig. 4a. The left dark brown solution is the Li_2S_6 polysulfide solution, which was made by adding Li_2S and S in the presence of a DOL/DME solution. As it is obvious in the right image, after adding the Co@KB composite after just two hours of contact, even with a high amount of
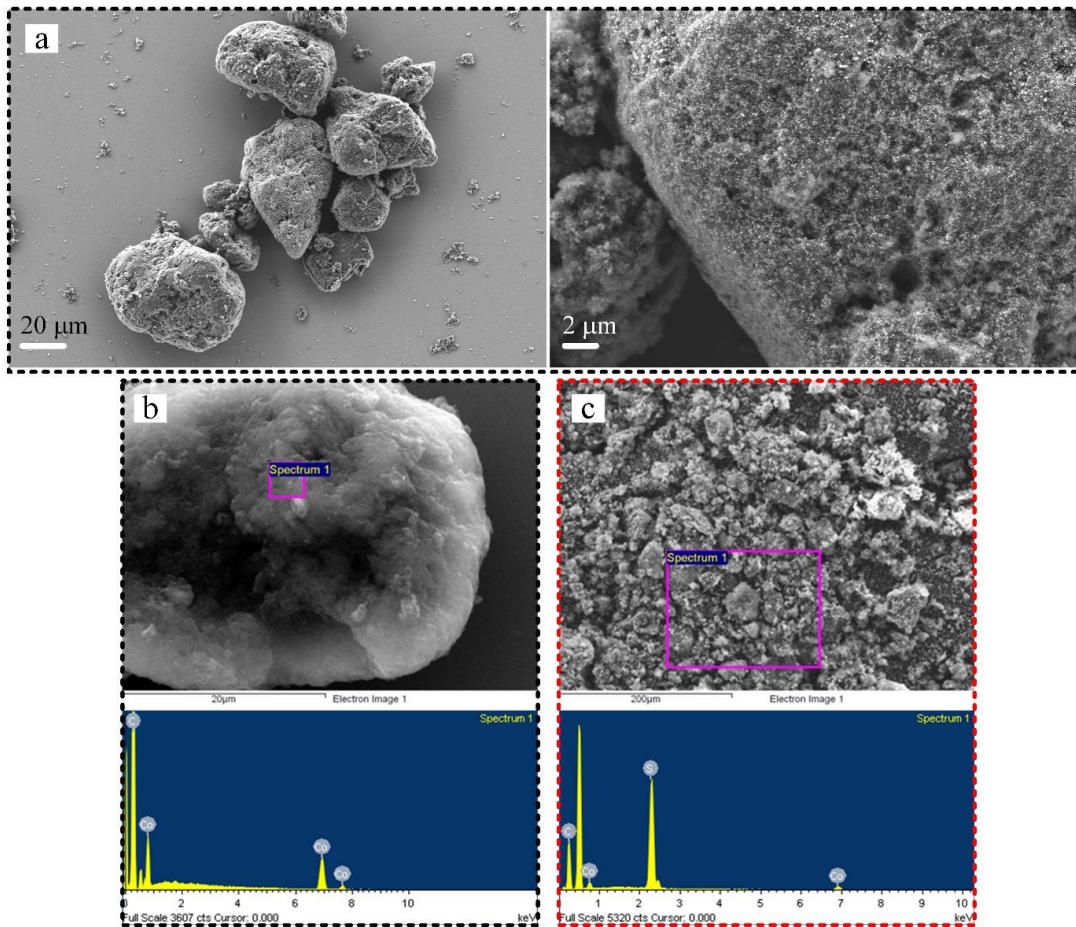
Fig. 3- (a) SEM image of Co@KB. SEM and corresponding EDX spectrum of (b) Co@KB and (c) Li_2S-Co@KB.

Li_2S_6, the color of the solution became lighter and more transparent, which shows the ability of the Co@KB composite to adsorb LiPSs [18]. Therefore, to analyze the electrochemical performances of the Li_2S-Co@KB composite, a lithium-sulfur battery was assembled in a coin cell with the as-prepared cathode, an ether-based electrolyte with $LiNO_3$ additive, which is good for LSBs, and a Li metal anode.

As shown in Fig. 4b, the Li_2S-Co@KB was charged and discharged between 1.7 and 3.6 V for the first activation cycle, and after that, the potential window changed to 1.7–2.8 V for the following cycles. Based on the previous reports [19], commercial and bulk Li_2S need around 4 V to fully decompose to sulfur in the first cycle. This high overpotential normally decomposes the ether electrolyte and decreases the LSB lifespan [20]. As depicted in Fig. 4b, the Li_2S-Co@KB composite has shown a smaller peak than 4 V in the activation barrier in the first charging curve, which suggests that the Co@KB composite promotes Li_2S activa-

tion. A lower overvoltage of about 3.4 volts in the Co@KB composite can prevent the decomposition of the ether-based electrolyte, facilitate the efficient transport of electrons within the cathode material, reduce resistive losses, and improve overall battery performance. Fig. 4b also reveals the charge-discharge curve for the second cycle; as is obvious, the activation barrier in the second cycle is almost removed. The Li_2S-Co@KB shows 850.3 and 760.3 $mAhg_{Li2S}^{-1}$ discharge capacities at 0.1 C for the first and second cycles, respectively. The high discharge capacity shows the high activation and utilization of the active material, which is also comparable to previously reported Li_2S-based LSBs (Table 1).

Furthermore, to assess the effect of the current rate on the discharge capacity, Fig. 4c shows the C-rate performance by applying the current from 0.1 to 5 C and returning to 0.2 C. As Fig. 4c shows the averaged discharge capacity of 733.7, 606.5, 554.9, 513.8, 450.9, and 368.3 $mAhg_{Li2S}^{-1}$ is achievable for 0.1, 0.2, 0.5, 1, 2, and 5 C, respectively. When the discharge current rate returned to
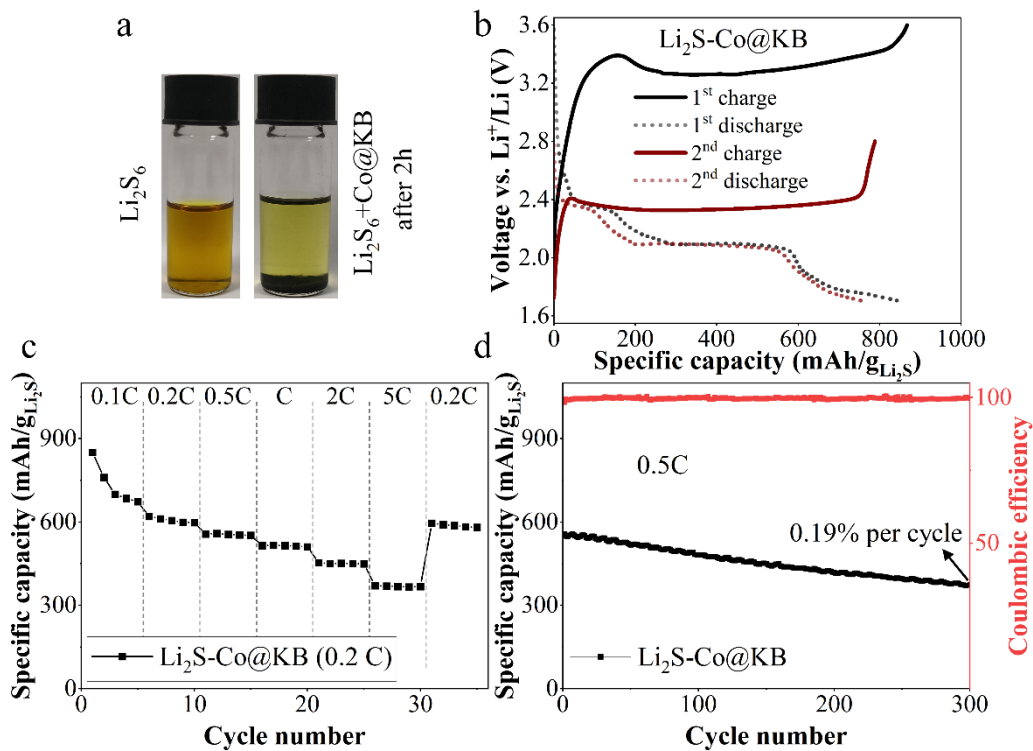
Fig. 4- (a) The digital photos of the Li_2S_6 solution and the LiPS adsorption ability of Co@KB. (b) Charging-discharging profiles of Li_2S-Co@KB electrode @ 0.1 C. (c) C-rate performances of Li_2S-Co@KB. (d) Cycling stability and Coulombic efficiencies of Li_2S-Co@KB electrode at 0.5 C.

0.2 C, a high discharge capacity of 587.5 mAhg$_{Li2S}^{-1}$ was recovered, which is around 96% of the first average capacity of the fresh cell at 0.2 C, demonstrating a good C-rate performance of Li$_2$S-Co@KB cathode. To assess the cycling performance, half-cells were cycled at a 0.5 C current rate after the first activation cycle. The Li$_2$S-Co@KB cell delivered a specific capacity of 558.7 mAhg$_{Li2S}^{-1}$ after activation and maintained 375.7 mAhg$_{Li2S}^{-1}$ at 300 cycles, corresponding to a low capacity fading of 0.19% per cycle (Fig. 4d). The improved conductivity ensures more uniform and efficient utilization of active materials, while the reduced overpotential barrier reduces energy losses and degradation during cycling. The cells at a moderate current rate of 0.5 C were prolonged for more than 300 cycles, which shows that the Co@KB composite can handle the shuttle effect by effectively chemically and physically trapping the polysulfides and efficiently utilizing the active materials, which bring excellent cyclability with good charge-discharge coulombic efficiency for the Li$_2$S-Co@KB cell. The combined effects of enhanced specific surface area and electrical conductivity, reduced overpotential barrier, and lower shuttle effect result in lower capacity fading and a longer cycle life for the Li$_2$S-Co@KB composite than the previously mentioned carbon-based host (Table 1).

Furthermore, to assess the effect of the current rate on the discharge capacity, Fig. 4c shows the C-rate performance by applying the current from 0.1 to 5 C and returning to 0.2 C. As Fig. 4c shows the averaged discharge capacity of 733.7, 606.5, 554.9, 513.8, 450.9, and 368.3 mAhg$_{Li2S}^{-1}$ is achievable for 0.1, 0.2, 0.5, 1, 2, and 5 C, respectively. When the discharge current rate returned to 0.2 C, a high discharge capacity of 587.5 mAhg$_{Li2S}^{-1}$

was recovered, which is around 96% of the first average capacity of the fresh cell at 0.2 C, demonstrating a good C-rate performance of Li$_2$S-Co@KB cathode. To assess the cycling performance, half-cells were cycled at a 0.5 C current rate after the first activation cycle. The Li$_2$S-Co@KB cell delivered a specific capacity of 558.7 mAhg$_{Li2S}^{-1}$ after activation and maintained 375.7 mAhg$_{Li2S}^{-1}$ at 300 cycles, corresponding to a low capacity fading of 0.19% per cycle (Fig. 4d). The improved conductivity ensures more uniform and efficient utilization of active materials, while the reduced overpotential barrier reduces energy losses and degradation during cycling. The cells at a moderate current rate of 0.5 C were prolonged for more than 300 cycles, which shows that the Co@KB composite can handle the shuttle effect by effectively chemically and physically trapping the polysulfides and efficiently utilizing the active materials, which bring excellent cyclability with good charge-discharge coulombic efficiency for the Li$_2$S-Co@KB cell. The combined effects of enhanced specific surface area and electrical conductivity, reduced overpotential barrier, and lower shuttle effect result in lower capacity fading and a longer cycle life for the Li$_2$S-Co@KB composite than the previously mentioned carbon-based host (Table 1).

4. Conclusions

In summary, the cobalt nanoparticles decorate the Ketjenblack with a facile and low-cost method that is effectively capable of increasing the electrical conductivity and decreasing the LiPSs shuttle effect by preventing the movement of polysulfides out of the composite during the discharge process. The Li$_2$S nanoparticles are introduced into the structure by a simple and safe liquid infiltration-evapora-

Table 1- A comparison of electrochemical performances of Li$_2$S-based cathodes

z	Electrolyte	Li$_2$S wt.%	Activation barrier@rate (1C=1166 mA g^{-1})	Initial discharge capacity (mAh g^{-1})@ rate
Li$_2$S-Co@KB (this work)	1.0 M LiTFSI in DME: DOL (v/v = 1/1) with 0.1 M of LiNO$_3$	61	3.39 @0.1 C	850.3@0.1C
Li$_2$S/graphene [21]	7.0 M LiTFSI in DME: DOL (v/v = 1/1)	82	3.5@0.05C	765@0.05C
Li$_2$S@porous carbon [22]	1.0 M LiTFSI in DME: DOL (v/v = 1/1) with 1wt% of LiNO$_3$	70	3.75@0.05C	772@0.05C
Li$_2$S-PAN [23]	3ml DMF solution of 6.4 mM naphthalene and 0.1 M LiNO$_3$	37	—	484@0.1C
Li$_2$S@C-CNT [24]	1.0 M LiTFSI in DME: DOL (v/v = 1/1) with 0.2 M of LiNO$_3$	—	2.63@0.1C	805@0.1C
nano-Li$_2$S/GA [9]	1.0 M LiTFSI in DME: DOL with 0.1 M of LiNO$_3$	69	~3.0@0.1C	838.5@0.1C

tion method, which can increase the conductivity of Li_2S particles and reduce the activation barrier of Li_2S. XRD, SEM-EDX, and optical adsorption tests of LiPS show that the cobalt nanoparticles distribute well and firmly in the KB. The galvanostatic charge-discharge curves show the ability of cathode active material to reduce the activation barrier and increase the utilization of active material, with a high initial discharge capacity of 850.3 $mAhg_{Li2S}^{-1}$ around 73% of the theoretical capacity of Li_2S) and high coulombic efficiency. The effect of increasing the current rate was also investigated with the C-rate test, and the results show a good response of the cathode to increasing the current rate. Furthermore, the Li_2S-Co@KB cathode shows a good cyclability at a 0.5 C current rate, with 0.19% of capacity fading per cycle over 300 cycles. The result shows that the low-cost and simple Co@KB composite has a good ability to adsorb the LiPSs and could be implemented to extend the cycle life of lithium-sulfur batteries.

Acknowledgments
Conflict of interest

References

1. Jiang J, Fan Q, Chou S, Guo Z, Konstantinov K, Liu H, Wang J. Li_2S-Based Li-Ion Sulfur Batteries: Progress and Prospects. Small. 2019;17(9).

2. Cárdenas B, Swinfen-Styles L, Rouse J, Garvey SD. Short-, Medium-, and Long-Duration Energy Storage in a 100% Renewable Electricity Grid: A UK Case Study. Energies. 2021;14(24):8524.

3. Wu F, Lee JT, Zhao E, Zhang B, Yushin G. Graphene–Li_2S–Carbon Nanocomposite for Lithium–Sulfur Batteries. ACS Nano. 2015;10(1):1333-40.

4. Xiang J, Zhao Y, Wang L, Zha C. The presolvation strategy of Li_2S cathodes for lithium–sulfur batteries: a review. Journal of Materials Chemistry A. 2022;10(19):10326-41.

5. Zhou L, Danilov DL, Eichel RA, Notten PHL. Host Materials Anchoring Polysulfides in Li–S Batteries Reviewed. Advanced Energy Materials. 2020;11(15).

6. Ye H, Li M, Liu T, Li Y, Lu J. Activating Li_2S as the Lithium-Containing Cathode in Lithium–Sulfur Batteries. ACS Energy Letters. 2020;5(7):2234-45.

7. Liang X, Yun J, Xu K, Xiang H, Wang Y, Sun Y, Yu Y. A multi-layered Ti_3C_2/ Li_2S composite as cathode material for advanced lithium-sulfur batteries. Journal of Energy Chemistry. 2019;39:176-81.

8. Wang D-h, Xie D, Xia X-h, Zhang X-q, Tang W-j, Zhong Y, et al. A 3D conductive network with high loading Li_2S @C for high performance lithium–sulfur batteries. Journal of Materials Chemistry A. 2017;5(36):19358-63.

9. Wang Z, Xu C, Chen L, Si J, Li W, Huang S, et al. In-situ lithiation synthesis of nano-sized lithium sulfide/graphene aerogel with covalent bond interaction for inhibiting the polysulfides shuttle of Li-S batteries. Electrochimica Acta. 2019;312:282-90.

10. He J, Chen Y, Manthiram A. Metal Sulfide-Decorated Carbon Sponge as a Highly Efficient Electrocatalyst and Absorbant for Polysulfide in High-Loading Li_2S Batteries. Advanced Energy Materials. 2019;9(20).

11. Qie L, Manthiram A. Uniform Li_2S precipitation on N,O-codoped porous hollow carbon fibers for high-energy-density lithium–sulfur batteries with superior stability. Chemical Communications. 2016;52(73):10964-7.

12. Li S, Jiang J, Dong Z, Wu J, Cheng Z, Zhu H, et al. Ferroconcrete-inspired construction of self-supporting Li2S cathode for high-performance lithium–sulfur batteries. Microporous and Mesoporous Materials. 2020;293:109822.

13. Jiang M, Liu G, Zhang Q, Zhou D, Yao X. Ultrasmall Li_2S-Carbon Nanotube Nanocomposites for High-Rate All-Solid-State Lithium–Sulfur Batteries. ACS Applied Materials & Interfaces. 2021;13(16):18666-72.

14. Xia M, Zhang N, Ge C. Mesoporous hollow carbon capsules as sulfur hosts for highly stable lithium–sulfur batteries. Journal of Materials Science. 2020;55(22):9516-24.

15. Zhang M, Yu C, Zhao C, Song X, Han X, Liu S, et al. Cobalt-embedded nitrogen-doped hollow carbon nanorods for synergistically immobilizing the discharge products in lithium–sulfur battery. Energy Storage Materials. 2016;5:223-9.

16. Liu Z, Zhou L, Ge Q, Chen R, Ni M, Utetiwabo W, et al. Atomic Iron Catalysis of Polysulfide Conversion in Lithium–Sulfur Batteries. ACS Applied Materials & Interfaces. 2018;10(23):19311-7.

17. Yang X, Li X, Adair K, Zhang H, Sun X. Structural Design of Lithium–Sulfur Batteries: From Fundamental Research to Practical Application. Electrochemical Energy Reviews. 2018;1(3):239-93.

18. Guo J, Omar A, Urbanski A, Oswald S, Uhlmann P, Giebeler L. Electrochemical Behavior of Microparticulate Silicon Anodes in Ether-Based Electrolytes: Why Does $LiNO_3$ Affect Negatively? ACS Applied Energy Materials. 2019;2(6):4411-20.

19. Li S, Leng D, Li W, Qie L, Dong Z, Cheng Z, Fan Z. Recent progress in developing Li2S cathodes for Li–S batteries. Energy Storage Materials. 2020;27:279-96.

20. Wan F, Fang L, Zhang X, Wolden CA, Yang Y. Lithium sulfide nanocrystals as cathode materials for advanced batteries. Journal of Energy Chemistry. 2021;63:138-69.

21. Wu F, Lee JT, Magasinski A, Kim H, Yushin G. Solution-Based Processing of Graphene– Li_2S Composite Cathodes for Lithium-Ion and Lithium–Sulfur Batteries. Particle & Particle Systems Characterization. 2014;31(6):639-44.

22. Wang N, Zhao N, Shi C, Liu E, He C, He F, Ma L. In situ synthesized Li_2S@porous carbon cathode for graphite/Li_2S full cells using ether-based electrolyte. Electrochimica Acta. 2017;256:348-56.

23. Shen Y, Zhang J, Pu Y, Wang H, Wang B, Qian J, et al. Effective Chemical Prelithiation Strategy for Building a Silicon/Sulfur Li-Ion Battery. ACS Energy Letters. 2019;4(7):1717-24.

24. Ye F, Noh H, Lee J, Lee H, Kim H-T. Li_2S/carbon nanocomposite strips from a low-temperature conversion of Li_2SO_4 as high-performance lithium–sulfur cathodes. Journal of Materials Chemistry A. 2018;6(15):6617-24.